Investigation of Piezoelectric Energy Harvesting From Structural Vibration Induced by Rotating Machinery

Hakan Ucar
Design Project Office, Istanbul, Turkey. E-mail: hakucar@ku.edu.tr

(Received 16 February 2022; accepted 30 June 2022)

Increasing energy consumption has led recent efforts towards energy harvesting technologies. Among them, piezoelectric energy harvesting with piezo-based sensors and energy harvesters have gained significant attention due to their applicability and efficacy for microscale power generation systems. Present study aims to investigate energy harvesting with piezoelectric materials from structural vibration propagating throughout the structure from vibration sources. For this purpose, a use case of a mechanical pump mounted on a steel foundation is chosen. A Finite Element (FE) model of the foundation of the pump with piezoelectric energy harvesters is developed and validated in an experimental setup. Measured frequency response functions (FRFs) show particularly good match with simulation results. Afterwards, a real measured acceleration data from the mechanical pump is applied. Simulations are performed and effectiveness of the piezoelectric energy harvester for two different locations are demonstrated. In this study, piezoceramic (PZT), PVDF polymer, ZnO film and a PMN-PT single crystal composite is considered as harvester material and the effectiveness of each piezoelectric material are compared.

1. INTRODUCTION

The use of fossil fuels such as oil, natural gas and coal for electricity generation leads to scarcity of natural raw material resources. Besides, it contributes significantly to environmental pollution. Therefore, research has recently started to find out alternative energy sources without leading any harm to the nature. Energy harvesting has the potential to play an alternative role especially for the low-energy electronics, and therefore harvesting energy from the environment has lately become a very encouraging technology. The concept of energy harvesting basically includes the direct conversion of ambient energy into electrical energy through some specific mechanisms. The ambient energy exists in various forms such as fluid,[1,2] solar,[3,4] wind,[5,6] wave[7,8] and vibration.[9,10] Among these energy forms, owing to its wide availability vibration energy has been widely investigated.

Machine vibration is one of the most existent and useful ambient energy sources easily found in marine and air platforms, vehicles, and production facilities. Although vibration and noise might threaten structural strength, they can be considered as potential regeneration energy resource for micro-scale sensor networks. One of the most important sources of vibration and noise is the structural vibration emitted from the machines. The vibration is propagated through its foundation and mountings to the surrounding structure. To establish a proper habitability and prevent the structural failure, vibration reduction measures such as vibration isolators and pads are applied. Even though, the vibration propagation cannot be fully avoided and structure-borne noise radiation from the structure is generated, which is an unfavorable situation. However, it can be possible to make use of this adverse condition by harvesting energy from undesired structural vibration.

Mechanisms commonly used in vibration energy harvesting presently include electrostatic,[11,12] electromagnetic,[13,14] magnestrictive,[15,16] triboelectric[17,18] and piezoelectric[19,20] materials. Among them, mechanical vibration energy harvesting using piezoelectric materials has received much attention due to its availability, simplicity, ease of integration and relatively high energy density. Piezoelectric energy harvesting of vibration usually applicable for harvesting low-level energy to power low-power electronics on the order of microwatts to milliwatts.[21]

State-of-the-art piezoelectric materials can be classified into four groups including ceramics, single crystals, polymers, and piezoelectric thin films. Piezoelectric ceramics, lead zirconate titanate (PZT), have been widely used owing to their direct coupling properties, excellent piezoelectric properties, and their capability to output large voltages. However, PZT materials can exhibit brittle fracture under heavy operational loads.[22] On the other hand, piezoelectric single crystals such as lead magnesium niobate-lead titanate (PMN-PT) and lead (P) indium niobate–lead magnesium niobate–lead(P) titanate (PIN-PMN-PT) have been developed to obtain better coupling through uniform dipole alignment.[23,24] In addition to ceramics and crystals, organic polymer materials such as polyvinylidene fluoride (PVDF) and polyimide, have lately gained significant interest with various advantages such as high piezoelectric constant, high dielectric strength, wide frequency response, low acoustic impedance, excellent mechanical flexibility, and low cost.[25,26] More recently developed zinc oxide (ZnO) thin films have many advantages such as no environmental pollution, no necessity for poling and a higher mechanical quality factor.[27,28]

There have been numerous studies recently carried out in the field of vibration-based energy harvesting via piezoelectric materials. Kim et al.[29] presented a closed form solution for harvesting energy efficiency of piezoelectric vibration energy harvesting system with a case study composed of a cantilever piezoelectric harvester. In other respects, Rajora et al.[30] investigated vibration-based energy harvesting by using a simply supported beam with a bonded piezoelectric patch to the surface. Lu et al.[31] focused on numerical investigation of piezoelectric energy harvesting from a pavement system. By means of this numerical study, they provided the optimal design characteristics of the pavement system. Similarly, Machavarapu et al.[32] investigated piezoelectric energy harvesting from pedestrian movements with the use of real pedestrian data. Luan et al.[33] proposed a method to specify the optimal locations of piezoelectric patches for a point-driven beam. In another study, a numerical model of a Glass Fiber Reinforced Polymer (GFRP) cantilever beam with the piezoelectric materials, PZT and PVDF was considered for energy harvesting and a comparison of PZT and PVDF materials was presented.[34] Lee et al.[35] provided a shape optimization study for a cantilever type piezoelectric energy harvester by conducting numerical simulations. In this study, the cantilever harvester was subjected to vibration on the tip and PZT and PVDF layers were considered with different combinations of shapes. Zhu et al.[36] presented a numerical investigation for the vortex-induced vibration. They studied the effect of Reynolds number on the piezoelectric energy harvesting. Turkmen et al.[37] investigated energy harvesting via piezoelectric material integrated shoe by means of numerical simulations and parametric analyses. Costa de Oliveria et al.[38] focused on the micro-fabricated piezoelectric cantilever harvester. The micro-cantilever harvester was exposed to mechanical vibrations and the performance of the harvester was compared with the similar existing harvesters.

Most studies on the piezoelectric energy harvesting focused on cantilever harvesters subject to free tip excitations. However, there are not many studies concerning piezoelectric energy harvesting from the structural vibration radiated through rotating machinery. Present work focuses on the piezoelectric energy harvesting on a structure subjected to structural vibration loads. For this purpose, a case study consisting of a mechanical pump and its foundation is carried out. Structurally radiated vibration from the pump is used as the energy to be converted via the use of patches made of different piezoelectric materials. Hence, a comparison between the piezoelectric materials (PZT, PVDF, PMN–PT and ZnO) is also provided in terms of generated voltage outputs.

2. THEORY OF PIEZOELECTRIC ENERGY HARVESTING

Piezoelectric energy harvesting can be described as the capability of extracting electrical energy when the piezoelectric materials are exposed to either compression or tension. In other words, piezoelectric materials produce electric current due to mechanical strain energy. This phenomenon can be defined mathematically as a coupling between the elastic and electric fields. An electromechanical coupling model is composed of piezoelectric material, structural layer, and electrodes. The piezoelectric material is connected to the appropriate electrical circuit to obtain the electrical outputs such as voltage and power, as shown in Fig. 1. The input energy arises from base-excited mechanical vibrations.

Electromechanical coupling model for vibration induced piezoelectric energy harvesting is built based on the energy conservation law, piezoelectric constitutive equations, and

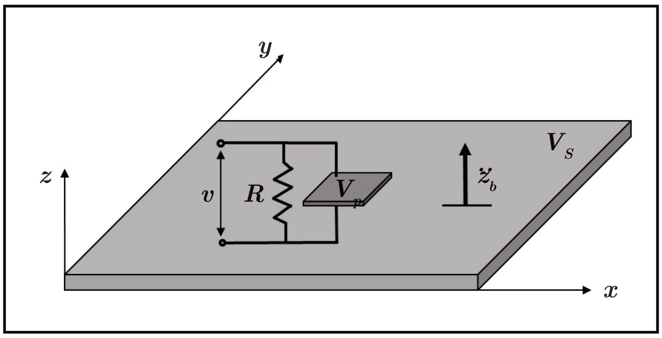

Figure 1. Schematic of a piezoelectric patch harvester attached on a substructure.

structural modal behavior.[39,40] According to the energy conservation law, electromechanical system can be defined as:

$$\int_{t_1}^{t_2} [\delta (T_k - U + W_e) + \delta W] dt = 0; \tag{1}$$

where T_k, U, W_e, W is kinetic energy, internal potential energy, electrical energy, and external work, respectively. These individual energy terms and work terms can be described as:

$$T_k = \frac{1}{2} \int_{V_s} \rho_s \, \dot{w}^t \, \dot{w} \, dV_s + \frac{1}{2} \int_{V_p} \rho_p \, \dot{w}^t \, \dot{w} \, dV_p; \tag{2}$$

$$U = \frac{1}{2} \int_{V_s} S^t \, \sigma \, dV_s + \frac{1}{2} \int_{V_p} S^t \, \sigma \, dV_p; \tag{3}$$

$$W_e = \frac{1}{2} \int_{V_p} E^t D \, dV_p; \tag{4}$$

$$\delta W = \sum_{k=1}^{nf} \delta w_k \, f_k(t) + \sum_{j=1}^{nq} \delta \varphi_j \, q_j; \tag{5}$$

where w is the displacement, V_s and ρ_s are the volume and the density of the host structure, respectively whereas V_p and ρ_p are the volume and the density of the piezoelectric patch connected to the structure, respectively. As shown in Eqs. 3 and 4, potential and electrical energies are determined with the stress, strain, and electric terms. Herein, S, σ, E and D denote the applied mechanical strain, generated stress, electric filed and obtained electric displacement, respectively. Superscript, t, here refers to the transpose of the matrix. As stated in Eq. 5, eternal work term is defined with the sum of work done by external forces at discrete locations and the charges,q_j obtained at discrete electrodes along with the electrode potentials, ϕ_j. Displacement of the structure, w can be written based on the standard modal transformation as the sum of kr individual mode shapes multiplied by the modal coordinate.

$$w\,(x, y, t) = \sum_{n=1}^{kr} \sum_{m=1}^{kr} \emptyset_{mn}\,(x, y) \;\, r_{mn}(t); \tag{6}$$

where w is the transverse displacement of the structure at position (x, y) and time, t, $\Theta_{mn}(x, y)$ is the mode shape function and r_{mn} is the modal time response is for the mn^{th} vibration mode.

S, σ, E and D are related to each other through material properties such as the permittivity of the piezoelectric element, ϵ, the piezoelectric coupling constant, e, and the elastic stiffness, c. Eq. 6 presents electromechanical constitutive equations.[41] Herein, superscript E represents constant electrical field while S stands for constant strain, where the elastic stiffness and permittivity parameters are determined.

$$\begin{Bmatrix} T \\ D \end{Bmatrix} = \begin{bmatrix} c^E & -e^t \\ e & \epsilon^S \end{bmatrix} \begin{Bmatrix} S \\ E \end{Bmatrix}. \tag{7}$$

Substituting Eqs. 6 and 7 into Eqs. 2 to 5 and rearranging of Eq. 1, two governing equations of motion are obtained as follows;

$$M\ddot{r} + C\dot{r} + Kr - \theta v = -F_b\,\ddot{z}_b; \tag{8}$$

$$\theta\dot{r} \;+\; C_p\dot{v} \;+\; \frac{1}{R}v \;= 0; \tag{9}$$

where r denotes the modal displacement, v is the electrical potential across the piezoelectric material. M, C, K, θ, C_p is the mass, damping, stiffness, coupling and capacitive matrix, respectively. Base acceleration due to the structural vibration, $\ddot{z}_b$ is the input to the electromechanical system. F_b is the forcing vector including inertial loads on the structure due to the base vibrations. A resistive electrical load, R is applied to harvest power from generated electrical potential, as presented in Eq. 9. To convert the modal responses to actual displacements, it is required to multiply them by the vibrational mode shapes. Thus, mass, stiffness, coupling and capacitive matrices are defined as follows;

$$M = \int_{V_s} [N_r]^T \rho_s [N_r]\, dV_s + \int_{V_p} [N_r]^T \rho_p [N_r]\, dV_p; \tag{10}$$

$$K = \int_{V_s} [B_r]^T [C_s] [B_r]\, dV_s + \int_{V_p} [B_r]^T \left[c^E\right] [B_r]\, dV_p; \tag{11}$$

$$C_p = \int_{V_p} [B_V]^T \left[\varepsilon^S\right] [B_V]\, dV_p; \tag{12}$$

$$\theta = -\int_{V_p} [B_r]^T [e] [B_r]\, dV_p; \tag{13}$$

where N_u and N_V is the matrix of displacement shape function and the matrix of electric potential shape function, respectively. B_r and B_V are the shape function derivatives defined by

$$[B_r] = \begin{bmatrix} \frac{\partial}{\partial x} & 0 & 0 & \frac{\partial}{\partial y} & 0 & \frac{\partial}{\partial z} \\ 0 & \frac{\partial}{\partial y} & 0 & \frac{\partial}{\partial x} & \frac{\partial}{\partial z} & 0 \\ 0 & 0 & \frac{\partial}{\partial z} & 0 & \frac{\partial}{\partial y} & \frac{\partial}{\partial x} \end{bmatrix}^T; \tag{14}$$

$$[B_v] = \begin{bmatrix} \frac{\partial}{\partial x} & \frac{\partial}{\partial y} & \frac{\partial}{\partial z} \end{bmatrix}^T. \tag{15}$$

3. NUMERICAL MODEL CONSTRUCTION AND VALIDATION

In this study, a mechanical pump, of which technical characteristics are given in Table 11, was considered as the vibration source. Machine vibration propagates from the mounts of the pump through the foundation and energy harvesting via two piezoelectric patches placed on the foundation was investigated. Frequency Response Functions (FRF) of the foundation were measured by using impact hammer to be used for the purpose of model validation. Vibration responses were measured as accelerations at each mount of the pump by means of the accelerometers, as illustrated in Fig. 2. Frequency of interest was taken up to 200 Hz, covering first the four orders of the pump. A representative response can be seen in Fig. 3 for the sensor number, 1 ($S1$).

Numerical model of the foundation with the piezoelectric patches was constructed as shown in Fig. 4. The location of the patches was determined by their exposure to high strains and their proximity to the pump. The corner point was selected as the Patch-1 location because more strain was expected at the corners of the foundation. On the other hand, Patch-2 location was chosen due its closeness to the pump.

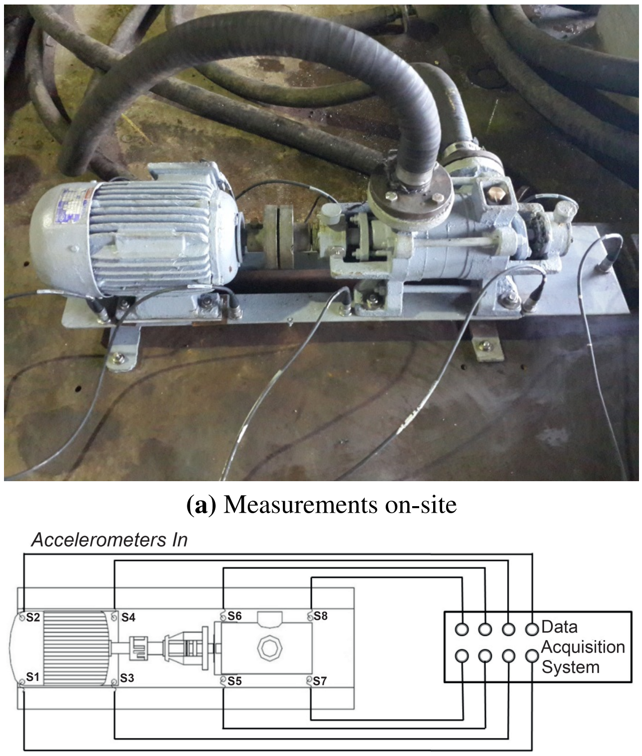

(a) Measurements on-site

(b) Schematic representation of measurement locations and system

Figure 2. Mechanical Pump.

Table 1. General characteristics of the pump.

Characteristics	Values
Speed	3000 rpm
Operating Voltage	380 V
Max. Pressure	10 bar
Input Power	15 kW
Foundation Material	AISI 304 Steel

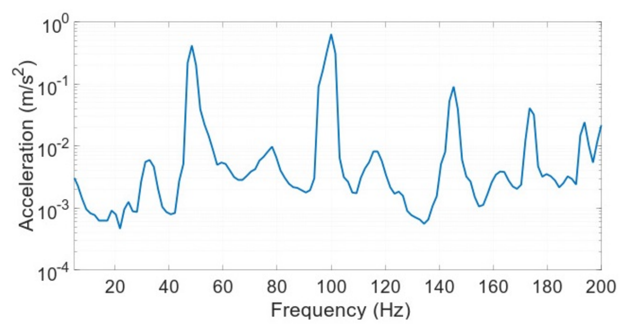

Figure 3. Response at Sensor #1.

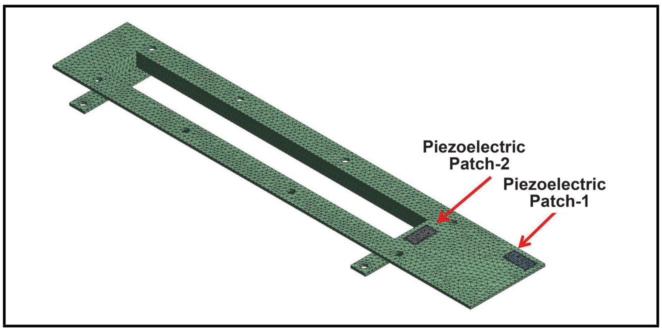

Figure 4. Finite element model of the pump foundation with piezoelectric patches.

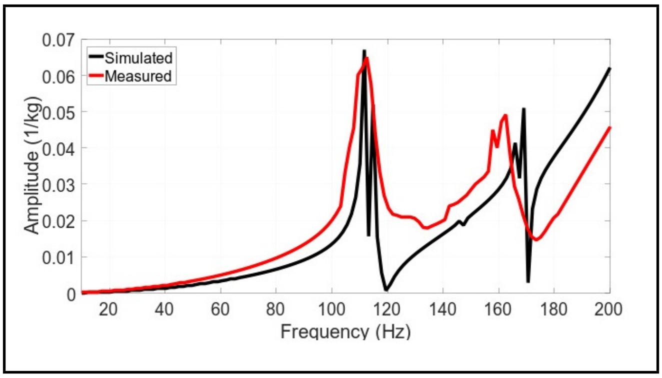

Figure 5. Experimental and numerical FRFs at the pump foundation.

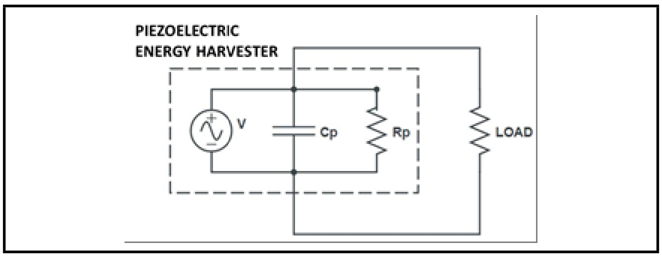

Figure 6. Simplified electrical circuit model.

To validate the numerical model to be used in energy harvesting study, the measured FRF of the structure was compared with the numerical FRF obtained from the model. As shown in Fig. 5, the simulated FRF catches the character of the measured one with admissible amplitude differences and there was an acceptable consistence between the measured and simulated results. Thus, it can be stated that the numerical model is valid to be used in piezoelectric energy harvesting study.

4. ENERGY HARVESTING STUDY

The electrical circuit of piezoelectric patch on the foundation was represented by a voltage source, V in parallel with internal capacitance C_p and internal resistance, R_p. A resistor was attached to the patch to harvest power. Therefore, the equivalent circuit model of the piezoelectric energy harvester with the resistive load, R is illustrated in Fig. 6.

Four different types of piezoelectric materials, PZT-5A, PVDF, ZnO and PIN24%-PMN-PT were used as the patch harvesters to perform a comparison study in terms of electrical outputs. These materials were assumed anisotropic while the pump foundation is considered isotropic.

Performance of energy harvesting strongly depends on the electromechanical properties of the piezoelectric materials. However, it should be noted that the piezoelectric strain coefficient, d is the most essential piezoelectric property in determining the effectiveness of piezoelectric materials for harvesting energy. A high value of d indicates a higher electrical output for a given applied strain. Two prevailing piezoelectric strain coefficients of piezoelectric materials were d_{31} and d_{33}. The d_{33} coefficient was the longitudinal coefficient which defines the electric polarization in the same direction with the applied stress. On the other hand, d_{31} coefficient was the transverse coefficient which describes the electric generation in a direction perpendicular to the direction of the applied stress.[42] In this study, the piezoelectric strain coefficient in the longitudinal mode d_{33} becomes prominent for energy harvesting since the base excitations are applied as compression forces on the piezoelectric material. The electromechanical properties of the piezoelectric materials used in this study are given in Table 2.

4.1. Generated Electrical Outputs

Measured accelerations at each 8 mounting locations were applied as the base excitation in the numerical model and the electrical outputs from the electromechanical system were obtained by performing harmonic analysis. In this section, the results with respect to the use of piezoceramic material (PZT-5A), which is widely used, were presented only. Same simulations were performed for all other piezoelectric materials and the results are given for the sake of comparison in the next section.

Since the voltage generated by the piezoelectric materials depends on the attached resistive load value, it is important to determine the optimal value of the resistive load that maximizes the harvested power. To accomplish this, the voltage and power versus resistive load curve should be obtained. The resistive load was varied in a wide range from 100 Ω to 1 MΩ. Figure 7 shows the peak values of electrical outputs with respect to resistive load values. According to Fig. 7, after a certain resistive load case, 100 kΩ, generated voltage remains almost constant while the harvested power tends to decrease. In this case, it can be stated that the open circuit condition ($R \to \infty$) is achieved. Thus, the optimal resistive load value is found to be 100 kΩ for which the Patch-1 delivered a maximum voltage of 0.41 V with a harvested power of 2.86 μW and a voltage of 2.99 V with a harvested power of 89.45 μW is obtained at Patch 2.

In Fig. 8, generated voltages with respect to connected resistive load and mechanical strain values at Patch-1 and 2 are shown. On the other hand, harvested power calculated from the effective voltage value generated for each resistive load value is presented in Fig. 9.

As mentioned before, the effectiveness of piezoelectric energy harvesting is closely related to mechanical strain occurred on the structure. It can be seen in Fig. 8 that there is high voltage generation in pump operating harmonics at where high strains occur. It has also been determined that higher voltage can be obtained from Patch-2, which is closer to the pump and subject to higher strains. Therefore, it can be stated that the harmonics of the pump is more dominant in voltage responses of Patch-2 compared to that of Patch-1.

Table 2. Fundamental electromechanical properties of piezoelectric materials.

Material	Density (kg/m^3)	Relative Dielectric Constant, ϵ_{33}	Piezoelectric Strain Constant, d_{33} (pC/N)	Elastic Constant, C_{33} (GPa)	Category	Reference
PZT-5A	7950	830	390	111	Soft ceramics	[43]
PVDF	1800	12.43	32.5	1.63	Polymer	[42]
ZnO	5665	8.31	12	233	Thin Film	[44]
PIN24%-PMN-PT	8122	868	1285	124.5	Single crystal composite	[45]

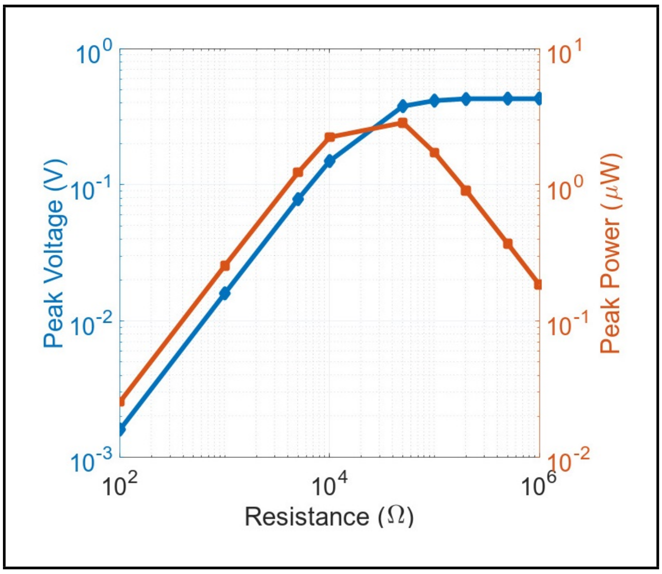

Figure 7. Peak electrical responses at PZT-5A based patches with respect to resistive loads.

4.2. Comparison of Different Piezoelectric Materials

In this section, different types of piezoelectric materials are considered for energy harvesting and compared in terms of obtained voltage outputs. These materials are, PZT-5A, PVDF, ZnO and PIN24%-PMN-PT, as mentioned before.

The results obtained with the use of mentioned piezoelectric materials are summarized in Table 3. According to the results, PIN24%-PMN-PT is specifically determined as the best piezoelectric material for energy harvesting among the other candidates. This is because PIN24%-PMN-PT composite has higher piezoelectric constant and dielectric constant compared to other piezoelectric candidates. PZT-5A ceramic emerges as the second one with a slight difference in terms of voltage generation. Finally, PVDF polymer and ZnO film take the last two places, respectively. However, PIN24%-PMN-PT composites have high brittleness under high mechanical force compared to that of other PZT ceramics.[46] Thus, they may not be suitable to be used under heavy loads. Besides, these composites are currently available in smaller size sheets resulting in higher cost. Consequently, PZT ceramics still come to the fore due to the small difference in voltage generation.

5. CONCLUSIONS

In this study, piezoelectric energy harvesting due to the structural vibration radiated from a pump through its foundation is investigated. Piezoelectric patches that can be used in complex structures are preferred instead of generally used cantilever-type harvesters. Two patches, one of which (Patch-2) is placed next to the pump mounts while the other one (Patch-1) is placed 15 cm away, are considered. Four different types of piezoelectric materials, PZT-5A ceramic, PVDF polymer, ZnO thin film and PIN24%-PMN-PT single crystal ternary composite are used as the patch harvesters to perform a comparison study in terms of electrical outputs.

Table 3. Summary of the energy harvesting results.

Parameter	PZT-5A	PVDF	ZnO	PIN24%-PMN-PT
Highest Voltage Output Location	Patch-2	Patch-2	Patch-2	Patch-2
Resistive Load (kΩ)	100	100	100	100
Peak Voltage (V)	2.9908	1.6378	0.1540	3.4275

First, frequency response functions (FRF) are measured from pump foundation via impact hammer. Then, acceleration data was measured by accelerometers while the pump was in operation. Finite element model of the electromechanical coupling involving pump foundation and piezoelectric patches was created and validated by comparing numerical and experimental FRFs.

Once the numerical model is validated, the piezoelectric harmonic analysis is performed with the input of measured base accelerations. According to the results of the harmonic analysis, satisfactory voltage outputs are obtained from the Patch-2, while the Patch-1 could not produce sufficient voltage. It is determined that the pump harmonics had a significant effect since the Patch-2 is close to the pump and higher strain occurs around Patch-2. Thus, it should be noted that effectiveness of piezoelectric energy harvesting is closely related to mechanical strain occurred on the structure. Consequently, it can be stated that prior to harvesting, numerical analysis should be performed with a validated model to determine the patch locations at where higher strains occur. Additionally, piezoelectric energy harvesting from structural vibration induced by rotating machinery is applicable with piezoelectric patches and generated electrical outputs can be supplied to low-energy electronics.

As far as the comparison between piezoelectric materials, it is determined that the highest voltage among the piezoelectric materials was generated with the use of PIN24%-PMN-PT. In terms of energy harvesting, the single crystal composite is followed by PZT-5A ceramic, PVDF polymer and finally ZnO film, respectively. However, PIN-PMN-PT composites are more fragile than PZT ceramics. Thus, they may not be

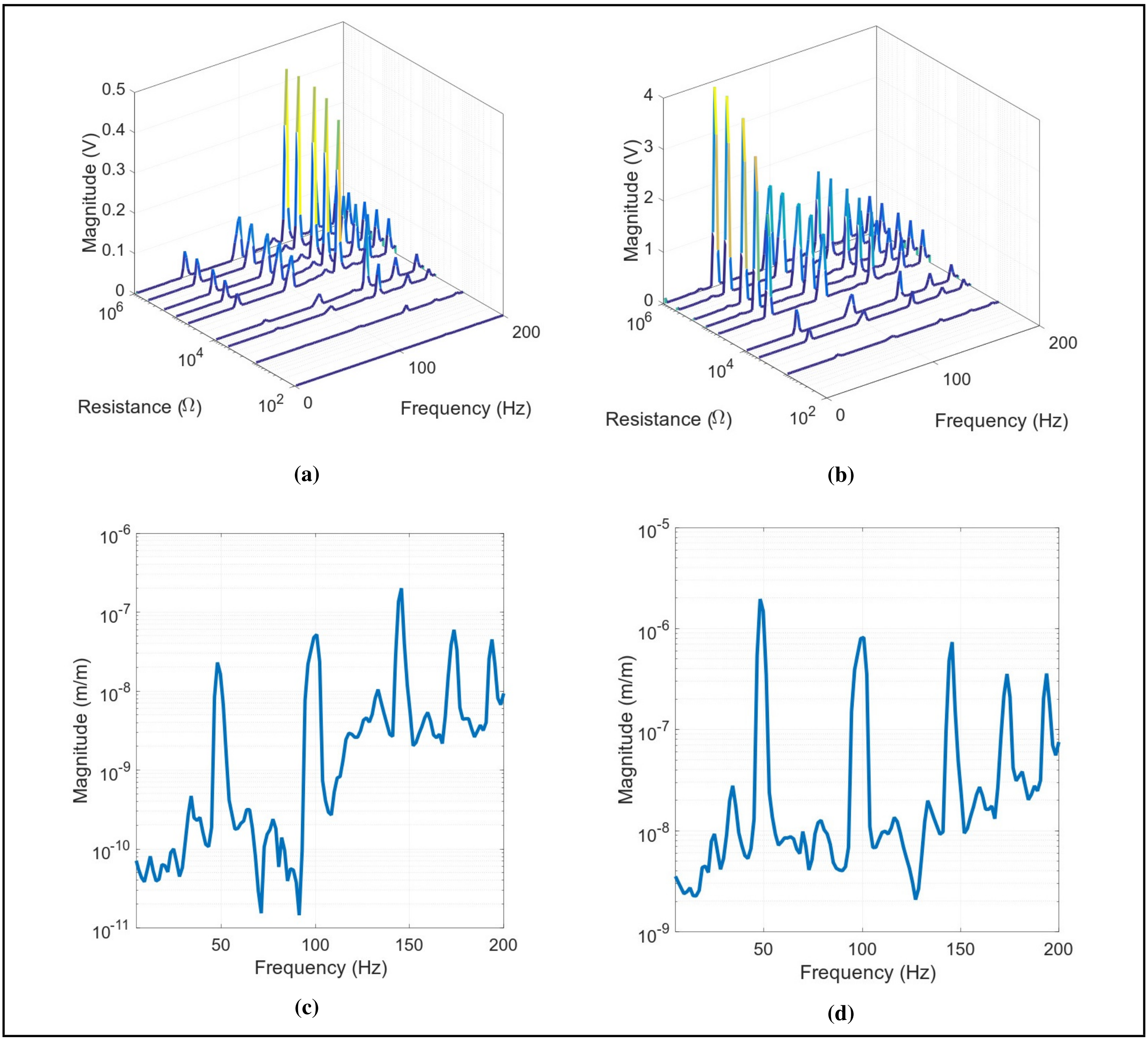

Figure 8. Simulation results at PZT based patches.

suitable to be used under heavy loads. Moreover, these composites are currently existing in smaller size sheets and not cost effective. Consequently, PZT ceramics are more applicable since there is slight difference in electrical outputs compared to PIN-PMN-PT.

In this study, only two piezoelectric patches are considered, and the energy harvesting from structural vibration is investigated. In the future study, “work zones” will be created around the operational loads and the zones where piezoelectric patches can operate will be classified according to their degree of energy harvesting efficiency. Besides, further studies on the real engineering application composed of a rotating machinery and its foundation will be performed.

REFERENCES

1. Aranda, J.J.L., Bader, S., and Oelmann, B. A space-coiling resonator for improved energy harvesting in fluid power systems, *Sens. Actuators A: Phys.*, **29**, 58–67, (2019). https://doi.org/10.1016/j.sna.2019.01.022

2. Wang, J., Zhao, G., Xu, J., Duan, K., Zhang, M., and Zhu, H. Numerical analysis of hydroenergy harvesting from vortex-induced vibrations of a cylinder with groove structures, *Ocean Engineering*, **218**, 108219, (2020). https://doi.org/10.1016/j.oceaneng.2020.108219

3. Song, Y.S., Youn, J. R., Yu, C., and Park, J. Sustainable solar energy harvesting using phase change material (PCM) embedded pyroelectric system, *Energy Conversion and Management*, **253**, 115145, (2022). https://doi.org/10.1016/j.enconman.2021.115145

4. Zhao, Y.N., Li, M.L., Long, R., Liu, Z.C., and Liu, W. Dynamic modeling and analysis of an advanced adsorption-based osmotic heat engines to harvest solar energy, *Renew. Energy*, **175**, 638–649, (2021). https://doi.org/10.1016/j.renene.2021.05.010

5. Jing, B. and Hao, W. Vibration analysis of rotting wind blades based on piezoelectric materials, *Int. Jour-*

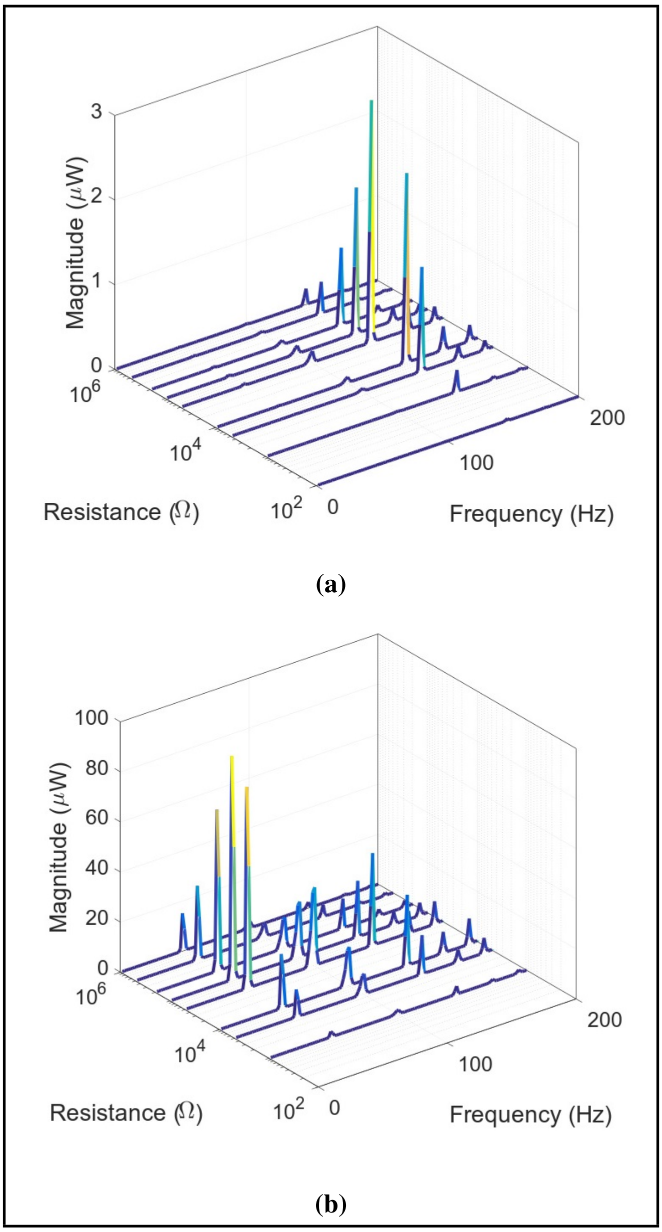

Figure 9. Harvested power at PZT based patches along with resistive loads.

nal of Acoustics and Vibration, **26**(1) 49–55, (2020). https://doi.org/10.20855/ijav.2020.25.11721

6 Zhou, Z., Pan, J., Qin, W., Zhu, P., Zhang, H., Du, W., and Deng, W. Improve efficiency of harvesting wind energy by integrating bi-stability and swinging balls, *Mechanical Systems and Signal Processing*,**170**, 108816, (2022). https://doi.org/10.1016/j.ymssp.2022.108816

7 Han, J., Maeda, T., Itakura, H., and Kitazawa, D. Experimental study on the wave energy harvesting performance of a small suspension catamaran exploiting the maximum power point tracking approach, *Ocean Engineering*, **243**, 110176, (2022). https://doi.org/10.1016/j.oceaneng.2021.110176

8 Ucar, H. Patch-based piezoelectric energy harvesting on a marine boat exposed to wave-induced loads, *Ocean Engineering*, **236**, 109568, (2021). https://doi.org/10.1016/j.oceaneng.2021.109568

9 Pereira, J.C. and Morangueira, Y.L.A. Energy harvesting assessment with a coupled full car and piezoelectric model, *Energy*, **210**, 118668, (2020). https://doi.org/10.1016/j.energy.2020.118668

10 Qin, W., Pan, J, Deng, W., Zhang, P., and Zhou, Z. Harvesting weak vibration energy by integrating piezoelectric inverted beam and pendulum, *Energy*, **227**, 120374, (2021). https://doi.org/10.1016/j.energy.2021.120374

11 De Queiroz, A.C.M. Energy harvesting using symmetrical electrostatic generators, *2016 ISCAS*, 650–653, (2016). https://doi.org/10.1109/ISCAS.2016.7527324

12 Zhang, Y., Wang, T., Luo, A., Huo, Y., Li, X., and Wang, F., Micro electrostatic energy harvester with both broad bandwidth and high normalized power density, *Applied Energy*, **212**, 362–371, (2018). https://doi.org/10.1016/j.apenergy.2017.12.053

13 Tan, Q., Fan, K., Tao, K., Zhao, L., and Cai, M. A two-degree-of-freedom string-driven rotor for efficient energy harvesting from ultra-low frequency excitations, *Energy*, **196**, 117107, (2020). https://doi.org/10.1016/j.energy.2020.117107

14 Asai, T., Araki, Y., and Ikago, K. Energy harvesting potential of tuned inertial mass electromagnetic transducers, *Mech. Syst. Sig. Process.*, **84**, 659–72, (2017). https://doi.org/10.1016/j.ymssp.2016.07.048

15 Fang, Z.W., Zhang, Y.W., Li, X., Ding, H., and Chen ,L.Q. Integration of a nonlinear energy sink and a giant magnetostrictive energy harvester, *J. Sound Vib.*, **391**, 35–49, (2017). https://doi.org/10.1016/j.jsv.2016.12.019

16 Wang, L. and Yuan, F. Vibration energy harvesting by magnetostrictive material, *Smart Mater. Struct.*, **17**, 045009, (2008). https://doi.org/10.1088/0964-1726/17/4/045009

17 Kwak, S.S., Yoon, H.J., and Kim, S.W. Textile-based triboelectric nanogenerators for self-powered wearable electronics, *Adv. Funct. Mater.*, **29**(2), (2019). https://doi.org/10.1002/adfm.201804533

18 Lai, Y.C., Li, L., Chen, Y.T., and Hsiao, Y.C. Mycena chlorophos-inspired autoluminescent triboelectric fiber for wearable energy harvesting, self-powered sensing, and as human–device interfaces, *Nano Energy*, **94**, 106944, (2022). https://doi.org/10.1016/j.nanoen.2022.106944

19 Erturk, A. and Inman, D.J. *Piezoelectric energy harvesting*, John Wiley & Sons, (2011).

20 Covaci, C. and Gontean, A. Piezoelectric energy harvesting solutions: A review, *Sensors*, **20**, 3512, (2020). https://doi.org/10.3390/s20123512

21 Safaei, M., Sodano, H.A., and Anton, S.R. A review of energy harvesting using piezoelectric materials: state-of-the-art a decade later (2008–2018), *Smart Mater. Struct.*, **16**, R1, (2007). https://doi.org/10.1088/1361-665X/ab36e4

22 Sridhar, A. and Keip, M.A. A phase-field model for anisotropic brittle fracturing of piezoelectric ceramics, *International Journal of Fracture*, **220**, 221–242, (2019). https://doi.org/10.1007/s10704-019-00391-9

[23] Kim, J, Ji, J.H., Dhin, D.J., Yoon, S., Ko, Y.H., Cho, K.H., and Koh, J.H. 2-Dimensional rGO introduced PMN-PT and P(VDF-TrFE) flexible films for enhanced piezoelectric energy harvester. *Applied Surface Science*, **494**, 1000–1006, (2019). https://doi.org/10.1016/j.apsusc.2019.06.236

[24] Molla, D., Placzek, M., and Wrobel, A. Multiphysics modeling and material selection methods to develop optimal piezoelectric plate actuators for active noise cancellation, *Applied Sciences*, **11**, 11746, (2021). https://doi.org/10.3390/app112411746

[25] Derakhshani, M., Momenzadeh, N., and Berfield, T.A. Analytical and experimental study of a clamped-clamped, bistable buckled beam low-frequency PVDF vibration energy harvester, *Journal of Sound and Vibration*, **497**, 115937, (2021). https://doi.org/10.1016/j.jsv.2021.115937

[26] Fang, Y., Hu, Y., Kang, W., Xie, L., Qiu, L., and Jin, T. Piezoelectric poly (vinylidene fluoride) (PVDF) polymer-based sensor for wrist motion signal detection, *Applied Sciences*, **8**, 836, (2018). https://doi.org/10.3390/app8050836

[27] Kumara, B. and Kima, S.W. Energy harvesting based on semiconducting piezoelectric ZnO nanostructures. *Nano Energy*, **1**, 342–355, (2012). https://doi.org/10.1016/j.nanoen.2012.02.001

[28] Wang, X., Song, J., Liu, J., and Wang, Z.L. Direct-current nanogenerator driven by ultrasonic waves, *Science*, **316**, 102–105, (2007). https://doi.org/10.1126/science.1139366

[29] Kim, M., Dugundji, J., and Wardle, B.L. Efficiency of piezoelectric mechanical vibration energy harvesting. *Smart Mater. Struct.*, **24**, 055006, (2015). https://doi.org/10.1088/0964-1726/24/5/055006

[30] Rajora, A., Dwivedi, A., Vyas, A., Gupta, S. and Tyagi, A. Energy harvesting estimation from the vibration of a simply supported beam, *Int. Journal of Acoustics and Vibration*, **22**(2), 186–193, (2017). https://doi.org/10.20855/ijav.2017.22.2463

[31] Guo, L. and Lu, Q. Numerical analysis of a new piezoelectric-based energy harvesting pavement system: Lessons from laboratory-based and field-based simulations, *Applied Energy*, **235**, 963–977, (2019). https://doi.org/10.1016/j.apenergy.2018.11.037

[32] Machavarapu, S., Karmakar, D., Majumdar, K., Pal, M., and Roy, P.K. Energy harvesting from pedestrian movement using piezoelectric material, *Materials Today: Proceedings*, **57**, Part 2, 391–397, (2022). https://doi.org/10.1016/j.matpr.2021.12.250

[33] Luan, X., Wang, Y., Jin, X., and Huang, Z. Optimal Locations of Piezoelectric Patch on Wideband Random Point-Driven Beam for Energy Harvesting, *ASME. J. Vib. Acoust.*, **140**(1), 011014, (2018). https://doi.org/10.1115/1.4037508

[34] Vinayaga, K.K., Vasanthanathan, A., and Nagaraj, P. Finite element modeling of smart piezoelectric beam using ANSYS, *Materials, Today: Proceedings*, **5**, 7078–7085, (2018). https://doi.org/10.1016/j.matpr.2017.11.372

[35] Lee, S., Park, J., and Kwak, B.M. Design optimization of piezoelectric energy harvester subject to tip excitation, *Journal of Mechanical Science and Technology*, **26**, 137–143, (2012). https://doi.org/10.1007/s12206-011-0910-1

[36] Zhu, H., Zhang, M., Zhang, C., Abdelkefi, A., Yu, H., Gaidai, O., Qin, X., and Wang, J. Piezoelectric energy harvesting from vortex-induced vibration of a circular cylinder: Effect of Reynolds number. *Ocean Engineering*; **235**, 109378, (2021). https://doi.org/10.1016/j.oceaneng.2021.109378

[37] Turkmen, A.C. and Celik, C. Energy harvesting with the piezoelectric material integrated shoe, *Energy,* **150**, 556–564, (2018). https://doi.org/10.1016/j.energy.2017.12.159

[38] Costa De Oliveria, F.A., Monteiro, D.W.D.L., and Colombo, D.M. Design, modeling, characterization and analysis of a low frequency micro-fabricated piezoelectric cantilever for vibration sensing and energy harvesting applications, *Sensors and Actuators A: Physical,* **326**, 112709, (2021). https://doi.org/10.1016/j.sna.2021.112709

[39] Kim, M., Hoegen, M., Dugundji, J., and Wardle, B.L. Modeling and experimental verification of proof mass effects on vibration energy harvester performance, *Smart Mater. Struct.,* **19**, 045023, (2010). https://doi.org/10.1088/0964-1726/19/4/045023

[40] Du Toit, N.E. and Wardle, B.L. Experimental verification of models for microfabricated piezoelectric vibration energy harvesters. *AIAA J.*, **45**, 1126–37, (2007). https://doi.org/10.2514/1.25047

[41] IEEE Standard on Piezoelectricity ANSI/IEEE Std 176-1987, ed, (1988).

[42] Ramadan, K.S., Sameoto, D., and Evoy, S. A review of piezoelectric polymers as functional materials for electromechanical transducers, *Smart Mater. Struct.*, **23**, 033001, (2014). https://doi.org/10.1088/0964-1726/23/3/033001

[43] Piezo.com. Materials Technical Data (Typical Values)—Piezo.com, https://info.piezo.com/hubfs/Data-Sheets/piezo-material-properties-data-sheet-20201112.pdf, (Accessed February 16, 2022).

[44] Pan, C.T., Liu, Z.H., Chen, and Y.C. Study of broad bandwidth vibrational energy harvesting system with optimum thickness of PET substrate, *Current Applied Physics*, **12**, 684–696, (2012). https://doi.org/10.1016/j.cap.2011.10.005

[45] CTS Corporation. Piezoelectric PMN-PT Single Crystal Products, https://www.ctscorp.com/wp-content/uploads/2016.12.15-Single-Crystal-Brochure.pdf, (Accessed February 16, 2022).

[46] Xu, S., Yeh, Y., Poirier, G., McAlpine, M.C., Register, R.A., and Yao, N. Flexible piezoelectric PMN-PT nanowire-based nanocomposite and device, *Nano Lett.*, **13**, 2393–2398, (2013). https://doi.org/10.1021/nl400169t